CURRENT SENSORS

REFERENCE DESIGN GUIDE

Application Note

TABLE OF CONTENTS

1 Introduction

Current sensing has become more and more important in the modern world. Many applications, such as traction inverters, electric motors, ACDC and DCDC converters, on-board chargers, battery management systems, and many others, are relying on current sensing to improve efficiency and safety. Melexis offers a wide portfolio of current sensors. In this document, we are going to present the high current sensing solutions of melexis: IMC-Hall® and Conventional Hall sensors, together with examples of assembly structures, and suggestions on how to design and build a current sensing module. This guide is divided in 5 main sections:

1. **Hall-effect current sensors:** an introduction to hall effect sensors, with some basic theory.
2. **Conventional Hall sensors**: a description of Conventional Hall sensors, with some insight on how to obtain an optimal design.
3. **IMC-Hall® sensors**: a description of IMC-Hall® sensors, an advanced technology enabling simple assembly. This section will also focus on examples and tips to reach the optimal design.
4. **Ferromagnetic materials**: a description of ferromagnetic materials used in a current sensing module, with also a focus on some assembly solutions.
5. **End-of-line calibration**: a description on how to reduce at minimum errors, to obtain the best design for your application.

2 Hall-effect current sensors

2.1 Hall effect

The Hall effect is named after the physicist Edward Hall who discovered it in 1879. It is based on the voltage difference arising between two extremities of a current conductor, when a current is flowing in it and a magnetic field is applied perpendicularly (Figure 1).
The charges flowing inside the current conductor (Hall element) are subjected to the Lorentz force caused by the magnetic field B, and drifted perpendicularly to the current flow I_H. Due to charges accumulation on the sides of the conductor, a voltage (Hall voltage V_H) is generated, that is proportional to the magnetic field, following Equation 1, where n is the charge density, q is the electron charge and d is the material thickness.

$$V_H = \frac{I_H}{nqd} B = S_H B \qquad \text{Equation 1}$$

$S_H = \frac{I_H}{nqd}$ is the Hall sensitivity. Equation 1 is based on a metal conductor. A semiconductor will need a different equation, since there are 2 different charge carriers: holes and electrons. However, the general conclusions can be drawn: the Hall sensitivity increases with the increase of the Hall current, and with the decrease of the charge carriers density and of the thickness of the material.

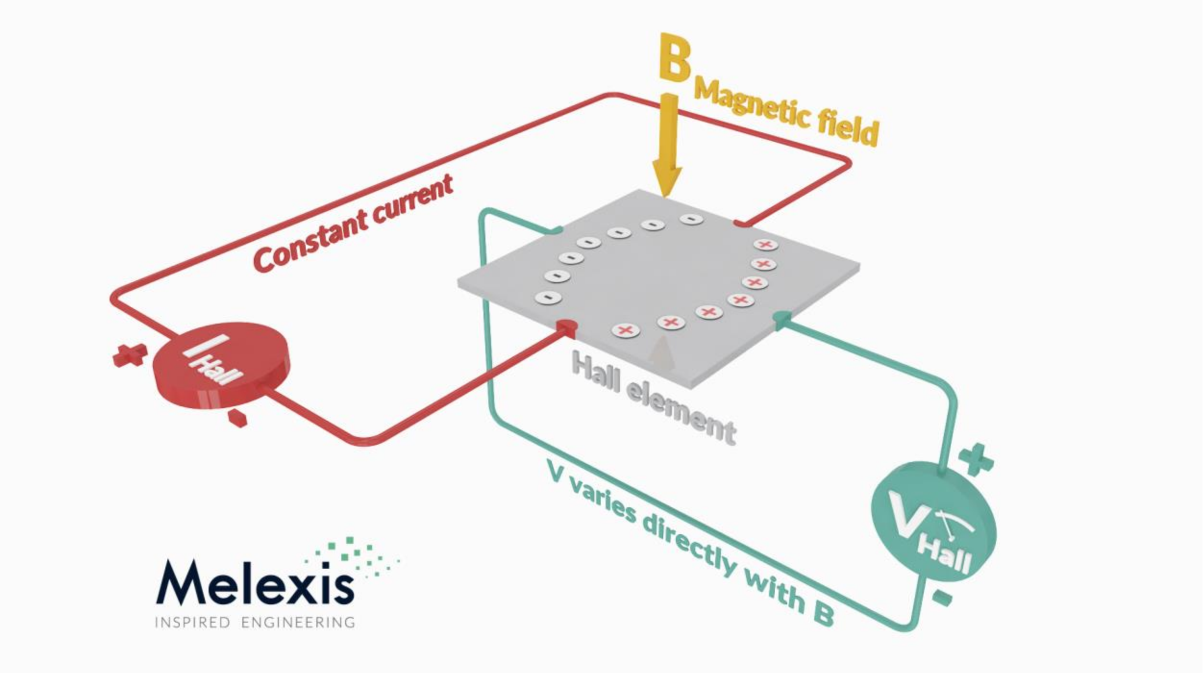

Figure 1: Scheme showing the Hall effect.

2.2 Hall effect current sensors

In Melexis current sensors, the current conductor is a silicon surface, integrated on the silicon IC. When it approaches a wire with a current flowing inside, it is subjected to the resulting magnetic field, that can be calculated thanks to Equation 2.

$$B = \frac{\mu_0 I}{2\pi r} \qquad \text{Equation 2}$$

Where r is the distance from the conductor and μ_0 is the vacuum permeability. This field can be substituted into Equation 1, obtaining the link between the Hall voltage and the current inside the wire (Equation 3).

$$V_H = S_H \frac{\mu_0}{2\pi r} I = S_H \cdot FF \cdot I \qquad \text{Equation 3}$$

The parameter $FF = \frac{\mu_0}{2\pi r}$ is the field factor. For geometries different than a wire, the field factor is computed with different equations, and in general it is equal to the ratio between the field and the generating current ($FF = B/I$). Normally, the farther is the sensor from the conductor, the smaller the signal will be.

Signal processing plays a fundamental role in the quality of the sensor. Thanks to the integration of the Hall element on a CMOS processed silicon IC, we can take advantage of integrated circuits for signal variable amplification (to obtain the desired sensitivity), offset and sensitivity correction and temperature compensation.

To concentrate the magnetic field on the sensor, and also to reduce the influence of external fields, it is possible to use ferromagnetic elements (cores and shields).

2.3 Types of Hall sensors used with ferromagnetic materials

2.3.1 Conventional Hall sensors

Conventional Hall current sensors (Figure 2) are sensitive to the magnetic field **perpendicular** to the chip surface. They are meant to be used in combination with a ferromagnetic core. In a typical application, the core is wrapped around the current conductor and concentrates the magnetic flux on a small air gap (typically 2-5mm) where the sensor is inserted.

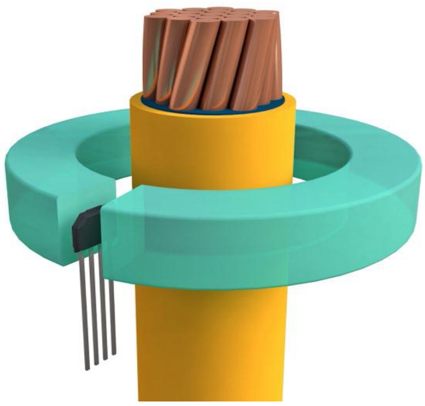

Figure 2: Conventional Hall sensor

Pros

- Strong magnetic gain from the core
- Very robust against cross-talk
- Suitable for medium to very high currents

Cons

- Performance limited by the core (geometry and material): saturation, hysteresis, frequency response and thermal drift
- Bigger footprint (size, weight) than solutions based on IMC-Hall® sensors

2.3.2 Planar IMC-Hall® sensors

The IMC-Hall® sensor (Figure 3) includes on top of the silicon IC a ferromagnetic layer (the Integrated Magnetic Concentrator, IMC) whose purpose is to concentrate the magnetic field on the sensing elements. Thanks to this technology, IMC-Hall® sensors are sensitive to magnetic fields **parallel** to the chip surface. Thus, the sensors can directly measure the current flowing in a bus bar or a PCB trace below the package, without the need for a core.

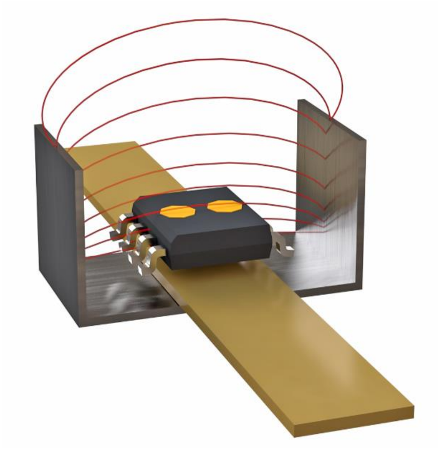

Figure 3: IMC-Hall® sensor

Pros

- Sensitive to magnetic field parallel to the chip surface, enabling an easy SMD assembly, vertical stacking and minimum footprint.
- IMC is made of magnetic material featuring very high permeability and very low hysteresis
- Magnetic gain from IMC

Cons

- Requires magnetic shielding or specific design to avoid cross-talk and/or noise from external fields

In the following document, we will discuss how to design at best a system with these 2 types of sensors.

3 Conventional Hall sensors

3.1 Introduction

Conventional hall sensors are typically enclosed in the air gap of a ferromagnetic core (circular or squared), wrapped around the current conductor (as shown in Figure 4. For a description of possible ferromagnetic materials, see section 5).

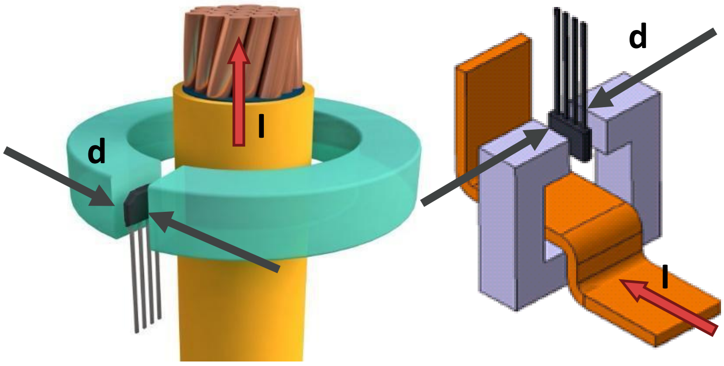

Figure 4: Example of mounting of conventional hall sensors.

The magnetic field B at the sensor position (in the center of the air gap), for a current I and a ferromagnetic core with air gap d, can be approximated as in Equation 4.

$$B\ [mT] = 1.25 \times \frac{I\ [A]}{d\ [mm]} \qquad \text{Equation 4}$$

The naming convention for ferromagnetic cores is C followed by the air gap dimension (for instance, C5 for a 5mm air gap shield). A development kit (link to application note on website) is available for designs testing.

3.2 Quick Selection Guide

Melexis provides a list of sensors that can be selected for different applications (Table 1). Each sensor can be bought with a factory trimmed sensitivity, using a specific option code. Sensitivity can be tuned according to customer needs.

	91209	91217	91219
Sensitivity [mV/mT] *	5-150	5-150	7-150
Thermal sensitivity drift [%S]	±1.5	±1	±1
Thermal offset drift [mV]	±10	±5	±5
Response time [µs]	2	2	2
Bandwidth [kHz]	250	250	400
Noise [mV_{rms}]	10	10	2
Analog output	Yes	Yes	Yes
Programmable	Yes	Yes	Yes
Diagnostic functions			
▪ Over/Under-voltage detection	Yes	Yes	No
▪ Broken-track detection	No	Yes	No
▪ Clamping	No	Yes	No
▪ Over Current Detection	No	No	Yes
Possible supply voltages [V]	5	5	5, 3.3
Package	SIP4-VA	SIP4-VA	SOIC-8/SIP4-VA
Operating temperature range [°C]	-40 to 150		

Table 1: Main features and specifications of conventional Hall effect current sensors. Values are typical. See datasheets for maximum limits.

** Programmable.*

Standard configurations are listed in Table 2. Updated list is available on datasheets.

Sensor	Option code	Sensitivity range (typical) [mV/mT]
MLX91209	CAA-000	5-150 (50)
	CAA-001	5-150 (15)
	CAA-002	5-150 (7.3)
	CAA-003	5-150 (19)
MLX91217	ACA-000	5-150 (10)
	ACA-001	5-150 (15)
	ACA-002	5-150 (17)
	ACA-003	5-150 (9)
	ACA-005	5-150 (13)
MLX91219	AAA-500	6.5-22.5 (7)
	AAA-501	6.5-22.5 (10)
	AAA-503	6.5-22.5 (15)
	AAA-504	16-55 (25)
	Generic part	5-105

Table 2: Option code and sensitivity range of conventional Hall effect current sensors. Please contact your local sales representative for customized versions.

For VA packages, different lead bending options are also available, to better match the mounting needs (see Figure 5). The shape can be selected by changing the third letter of the option code (for instance, to select a planar leads shape, the option conde for a MLX91219 should be AAZ instead of AAA). Table 3 resumes the length of the leads, and the reference points from which it is measured (described in Figure 6).

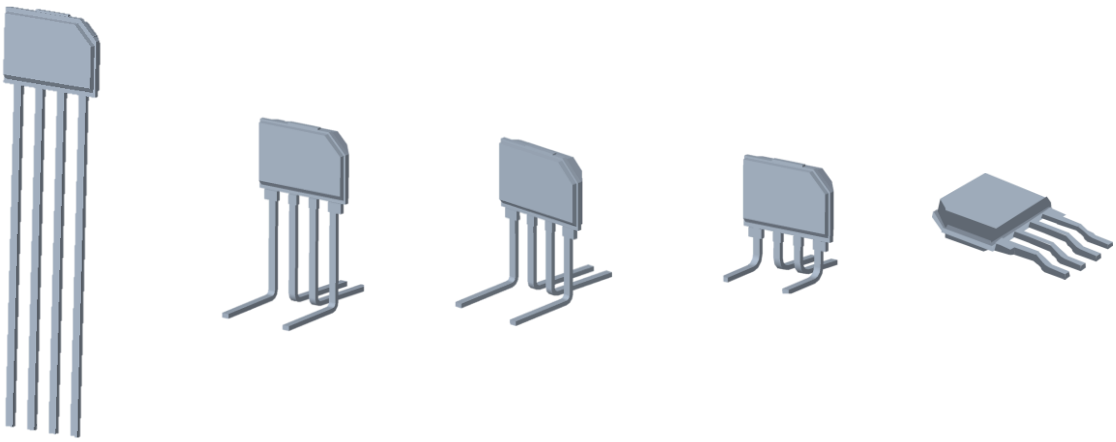

Option code: xxA	**Option code: xxR**	**Option code: xxS**	**Option code: xxT**	**Option code: xxZ**
(a)	(b)	(c)	(d)	(e)

Figure 5: Different leads bending options: (a) straight leads, (b, c, d) bent leads, (e) and planar leads.

Option code	Name	Reference point	Lead length [mm]
A	VA straight leg	Package	18
R	STD-2	Dambar	5.34
S	STD-3	Dambar	3.7
T	STD-4	Dambar	1.68
Z	SMD style	Dambar	2.15

Table 3: Dimensions for each different lead bending option.

Figure 6: example of reference distances for VA package.

In case customized dimensions are needed, please contact your local sales representative.

4 IMC-Hall® Sensors

IMC-Hall® sensors are based on an Integrated Magnetic Concentrator (IMC, a ferromagnetic layer placed on top of the silicon IC) that locally converts the horizontal magnetic field (B_x) into a vertical component (B_z) that can be measured by high performing silicon Hall elements. To concentrate the field on the sensor, and to protect it from external fields, ferromagnetic shield are normally used (see Figure 7).

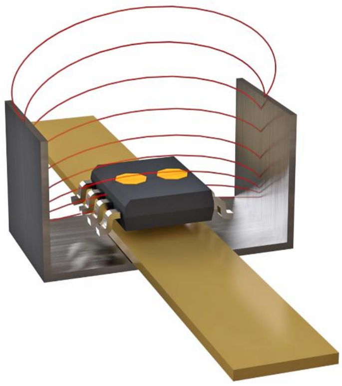

Figure 7: IMC-Hall® sensor. The yellow regions show the approximate position of the IMCs.

Figure 8 shows how a horizontal field is bent to be converted into a vertical field at the hall plates position (2 sensing points are present). This enables a differential sensing, rejecting any other field that is not parallel to the sensor plane. IMC are available in different types, as explained in section 4.1.

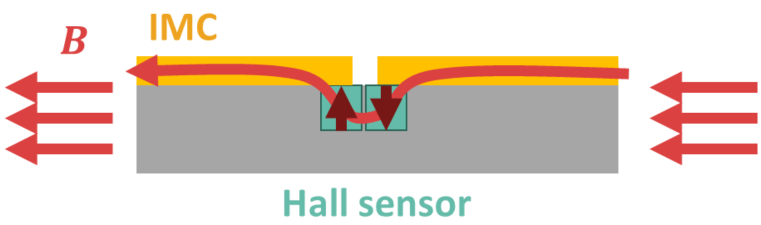

Figure 8: IMC and field bending. Any field in the Z direction is rejected by the differential sensing.

4.1 IMC versions

IMC-Hall® sensors are available in 4 different versions covering a broad range of sensitivities and magnetic field ranges: Low Field (LF), High Field (HF), Very High Field (VHF), Extra High Field (XHF). With its strong magnetic gain, the LF IMC is ideally suited for applications with low currents, requiring high magnetic sensitivities (up to 700mV/mT). At the other end of the scale, the XHF IMC can linearly sense strong magnetic fields up to ±90mT, for current sensing applications with very high-power densities. In the following pages, Figure 9 shows the different sensitivity ranges that IMCs can reach. Figure 10 shows the linearity ranges for each one of the IMCs, and Figure 11 shows the current ranges in which IMCs can be used.

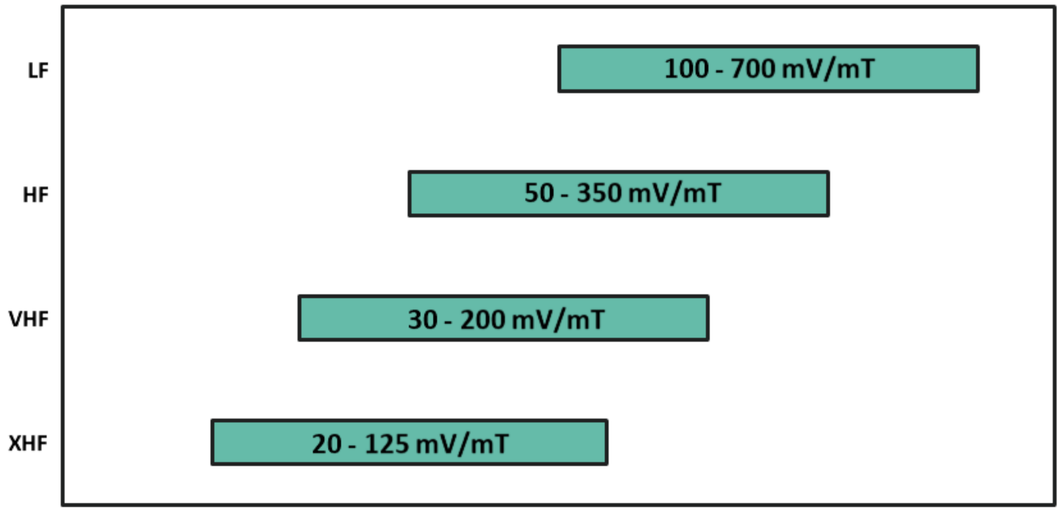

Figure 9: Sensitivity range of each IMC version.

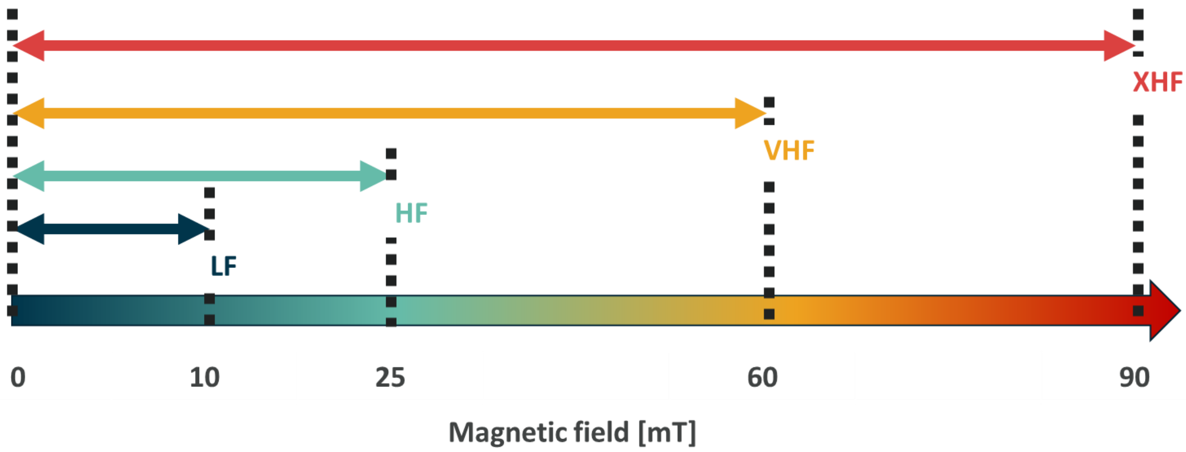

Figure 10: Linearity range for different IMC configurations.

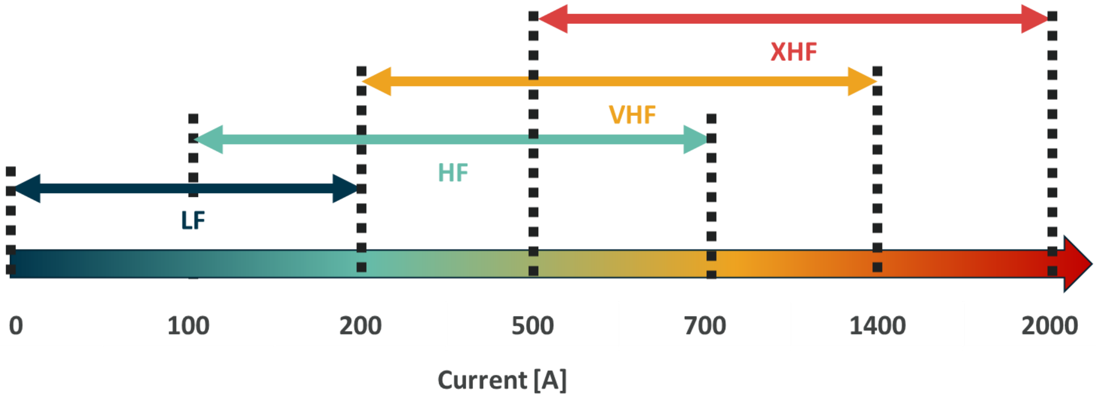

Figure 11: Optimal IMC configuration for different current ranges. Saturation of shields should also be considered. Melexis offers an online simulator tool, to choose the most optimized solution for a current sensing application, the current sensor simulator.

The design of the magnetic system around the sensor is important to be able to take advantage of the best performances of Melexis sensors.

4.2 Magnetic design

The next sections provide a guide for an optimal magnetic design of an IMC-Hall® sensing system. First, simple rules for magnetic field estimation will be described (section 4.2.1). Then, solutions will be described in order to improve signal to noise ratio and stray field immunity (sections 4.2.2 and 4.2.3), to increase frequency response and linearity (section 4.2.4), to remove the effect of mechanical tolerances (section 4.2.5), and finally to implement the IMC-Hall® sensor without ferromagnetic shields (sections 4.2.6 and 4.2.7). For a focus on the ferromagnetic materials, see section 5.

4.2.1 Magnetic field estimation

To compute the needed sensitivity, the magnetic field at the sensor location can be estimated, considering the configuration in which the IMC-Hall® sensor is used: with or without shield.

Magnetic field estimation with shield

In a typical application, a U-shaped ferromagnetic shield is wrapped around the current conductor to protect the sensor from external fields and improve the overall robustness of the sensing solution (see Figure 12).

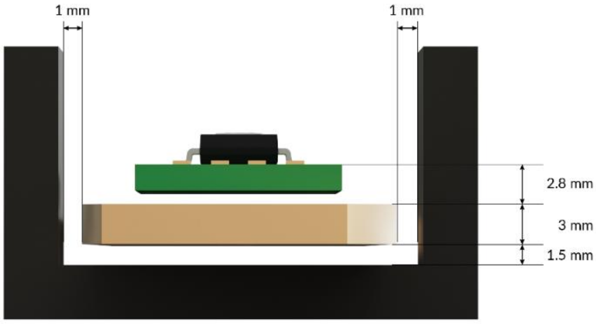

Figure 12: Shield and sensor assembly, with standard spacings.

The most important dimension of the shield is the inner width. In this configuration, the magnetic field B measured by the sensor for a current I and an inner width W can be estimated as:

$$B\ [mT] = 1.25 \times \frac{I\ [A]}{W\ [mm]} \qquad \text{Equation 5}$$

Figure 13 shows how dimensions are measured on a shield.

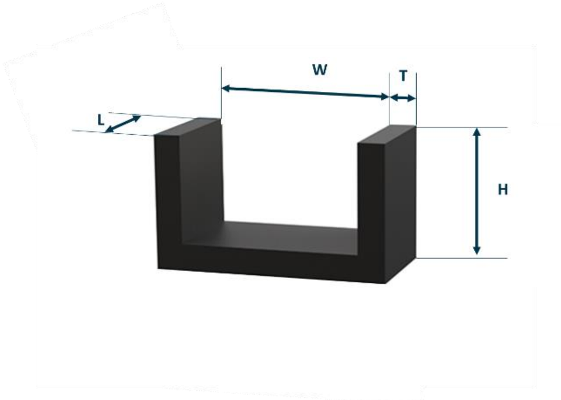

Figure 13: definition of dimensions of shields.

In order to have an increased signal-to-noise ratio, the sensor should be mounted at a certain depth inside the opening of the shield, where the field lines are quasi-parallel to each other, and therefore homogeneous. We suggest to follow the dimensions shown in Figure 12.
Typically, the shield thickness T ranges between 0.8 and 3 mm. The height H and length L are between 12 and 15 mm, in order to properly surround the sensor in each direction. The naming convention of ferromagnetic shields is U (for standard shields) or LU (for laminated shields) followed by the width number (for instance, L20). NiFe and SiFe are two available materials. Different properties are described in section 5.4.

Magnetic field estimation without shield

Depending on application environment and requirements, the ferromagnetic shield is not necessarily required. However, this configuration would lead to a drastic reduction of stray field immunity.

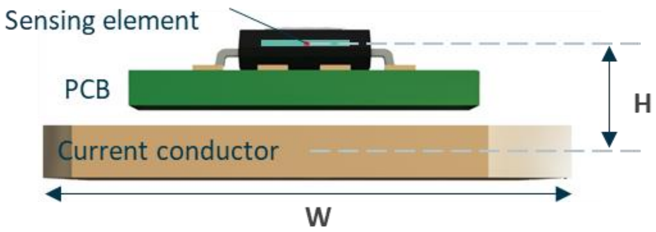

Figure 14: dimensions on sensor without shield.

Without shield, the magnetic field B measured by the sensor for a current I, a trace width W and a vertical position H can be approximated as:

$$B\ [mT] = 0.4 \times \frac{I[A]}{W[mm]} * \operatorname{atan}\left(\frac{W[mm]}{2H[mm]}\right) \qquad \text{Equation 6}$$

4.2.2 Conductor with neck-down

In order to limit the cost, size and weight of the shield on systems with wide bus bars, we recommend reducing its cross-section locally, as illustrated in Figure 15. Such a neck-down has minimal impact on the electrical resistance and allows for a much more compact current sensing solution.

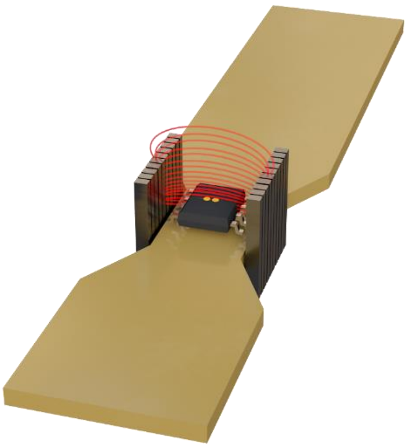

Figure 15: Necked-down bus bar example.

4.2.3 Stray field immunity

IMC Hall® sensors are protected from external or stray fields (i.e. fields that are not generated by the current under measurement) by shields. Stray fields can be generated by external sources or, in case of an inverter application, by the other phases, that should be measured by other sensors (cross talk). Stray fields can affect both offset (in case of a constant field, not related to the measured current) and sensitivity (when the external field changes with the measured current).

Stray field reduction

Stray field from an external source can be reduced first of all by increasing its distance with the sensor. Figure 16 shows how cross talk decreases with the increase of the distance. These simulated values are calculated for distances between 20mm and 170mm, with 2 cases: one with the sensor perfectly centred in the middle of the shield, and one with the sensor displaced in the horizontal direction by 1mm. It is possible to notice that a centred sensor represents the best configuration to minimize the stray field.

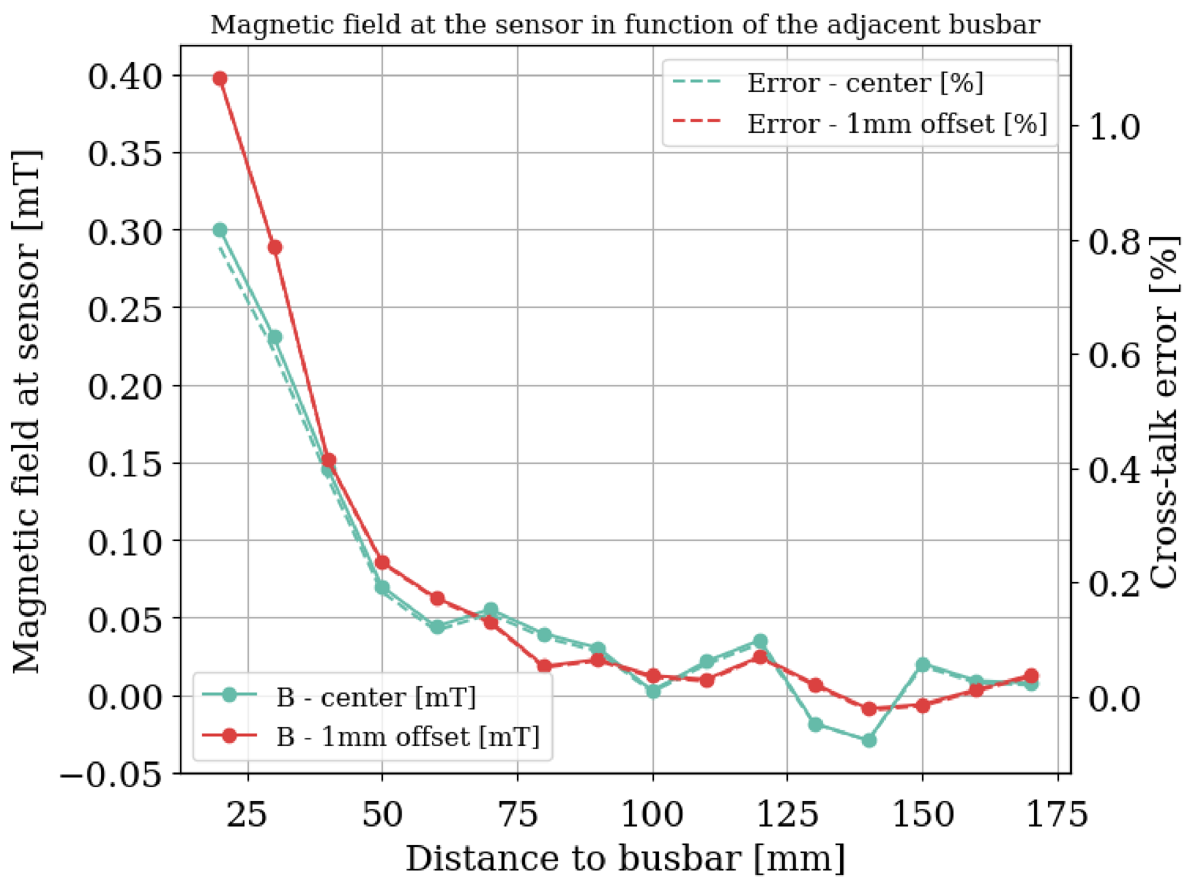

Figure 16: Cross talk error and stray field dependence with the increase of bus bar spacing.

Stray field rejection

When the distance cannot be increased enough to reduce the error from a stray field source, it is necessary to use the ferromagnetic shield properties. We saw that by decreasing the shield width, the field intensity on the sensor increases (Equation 5). Moreover, this also reduces the quantity of external field that reaches the sensor, or, in other words, increases the ratio between the external field B_{ext} and its component inside the shield B_{int}, called the Shielding factor $SF = B_{ext}/B_{int}$ (Figure 17).

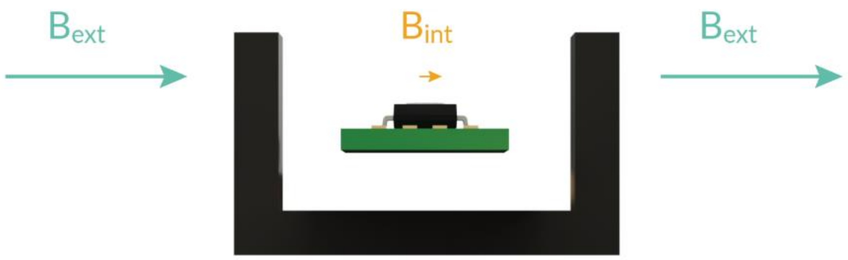

$$SF = \frac{B_{ext}}{B_{int}} [-]$$

Figure 17: Shield factor definition

Figure 18 shows how increasing the shield width reduces the shielding factor, leading to a larger influence from stray field sources. In case the shield width is limited by the bus bar dimensions, it is possible to adopt the necking down solution (see Figure 15), to locally reduce the bus bar thickness to be able to use small shields.

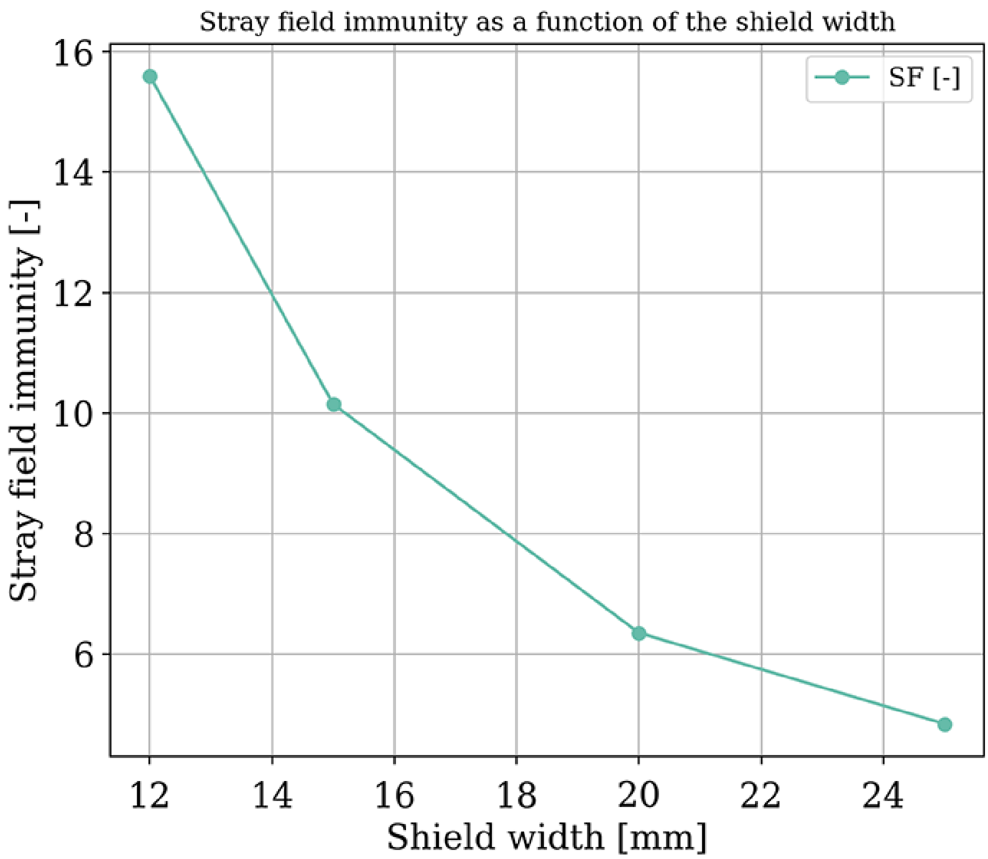

Figure 18: Shielding factor versus shield width.

4.2.4 Use of laminated shields

Laminated shields are made of a stack of thin sheets separated by insulators. This allows to reduce the effect of eddy currents (that are generated in the shield by time oscillating fields, and cause gain reduction and phase shift of the sensor signal), boosting the sensing performances. Moreover, for very high currents (typically above 800A), it is often more efficient and cost-effective to use a laminated shield so that the in-plane thickness can be increased, decreasing the depth and overall footprint for the same performance.

4.2.5 Mechanical tolerances and vibrations

The mechanical assembly of the sensor and shield has tolerances, that may affect the measurements of the system. Any static error can be compensated by end of line calibration (see section 6). However, vibrations will introduce a time variable error of the sensitivity, since movements of the sensor with respect to bus bar and shield affect directly the field factor. The influence of displacements in the three Cartesian directions is shown in Figure 19, while Figure 20 shows how the reference system is chosen on the bus bar and shield assembly.

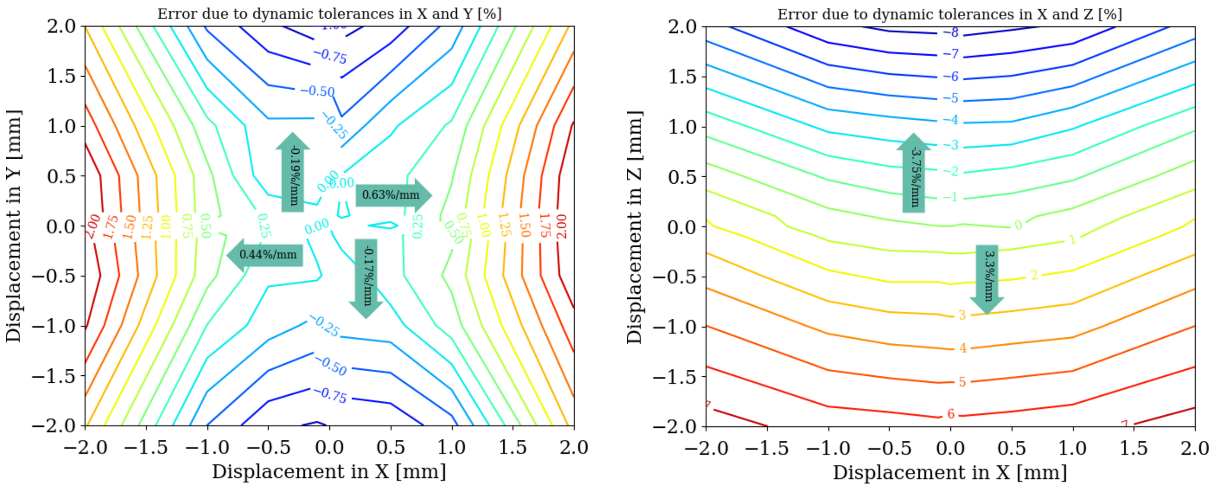

Figure 19: Effect of mechanical vibrations on the sensitivity.

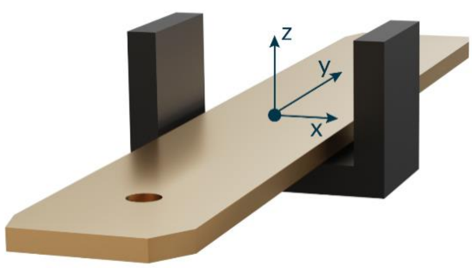

Figure 20: definition of reference system on the bus bar and shield assembly

From Figure 19 we can observe that displacements in the Z direction affect the most the sensitivity of the sensor. Displacements in X and Y directions influence less the error.
We can conclude that the IMC-Hall technology is very robust against mechanical tolerances in the X and Y directions. For an optimal design it is recommended to strengthen the fixation along the Z direction by placing the fixation screws close to the sensor and shield assembly.

4.2.6 Cancelling stray field without shield

In AC applications, external stray fields can be cancelled out by the microcontroller. Computing the difference between max and min sensor output values provides a signal independent of any parasitic DC field (see Figure 21).

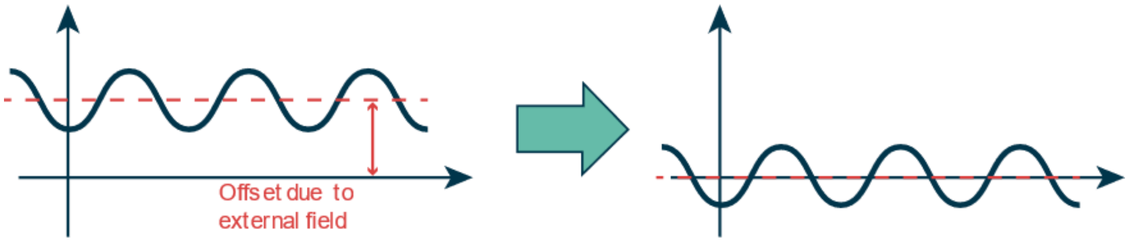

Figure 21: Stray field cancelling without shield.

4.2.7 Avoiding cross-talk without shield

Even without ferromagnetic shield, cross-talk between adjacent current tracks can be avoided by design. Figure 22 illustrates a concept of current trace layout with slots to force the current to flow perpendicular to the main track axis. The sensors are rotated by 90° with their sensitive axis (blue arrow) parallel to the current trace. With such a configuration, there is virtually no cross-talk between phases.

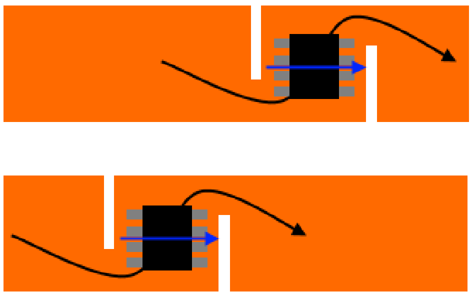

Figure 22: Current trace layout with slots and rotated sensors to avoid cross-talk between phases.

PCB design is also important to have an optimal current sensing solution. Section 4.3 shows some suggestions on how to optimally integrate the sensor and to design a PCB.

4.3 PCB design

The PCB design and layout play an important role in the final performances of the current sensing module. More specifically, two different aspects are to be considered when designing the ground layer on the PCB.
When an application implies high voltage switching (for instance in motor control applications), an expanded ground layer, as depicted in Figure 23, will help reducing the parasitic coupling capacitance generated by voltage time transients (dV/dt).

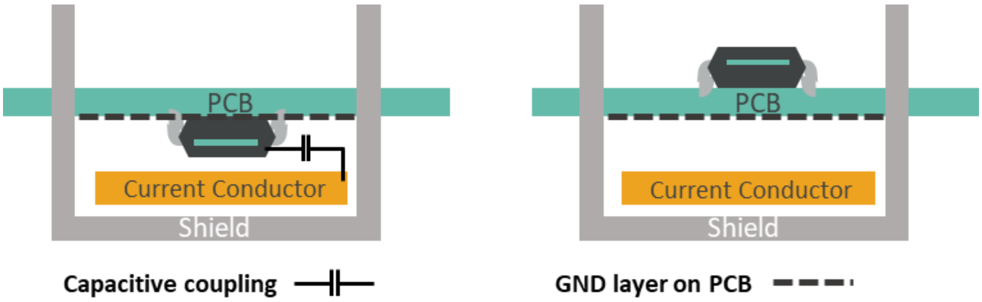

Figure 23: Current sensing structure. Expanded Ground Layer on PCB in order to reduce the parasitic coupling capacitance (coming from voltage transients).

At the same time, the ground layer can have a big impact on the response time.
If the ground layer covers all the surface of the PCB and surrounds the two legs of the shield, Eddy currents will start to flow circularly around them, generating a counter-magnetic field which slows down the response time of the sensor.
In order to avoid increased response time, the ground layer should be divided such that it interrupts the circulations of Eddy currents around the shield (see Figure 24).

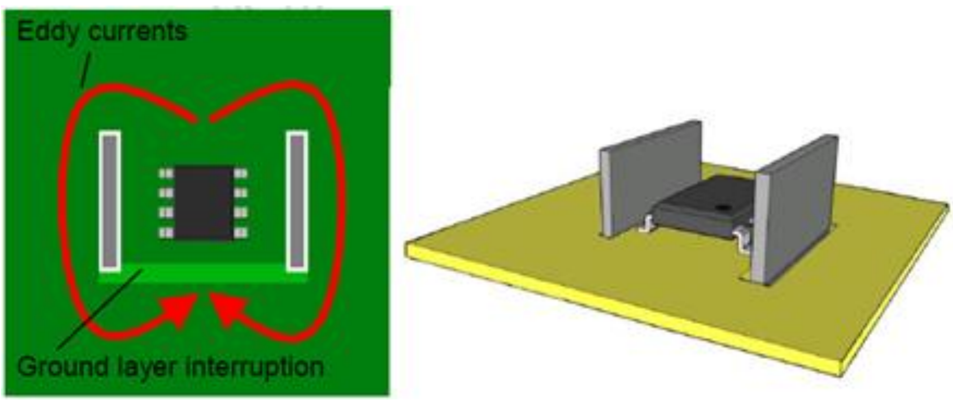

Figure 24: Current Sensing Structure – Designing the Ground Layer on the PCB such that Eddy Currents circulations is interrupted

4.4 Reference Designs

Table 4 shows an overview of reference designs based on IMC-Hall® current sensors for different target applications.

Application	Solution	Illustration
PCB trace current **2-10A**	Multi-turn and multi-layer PCB or single layer PCB with C-shaped ferromagnetic shield (section 4.4.1 and 4.4.2).	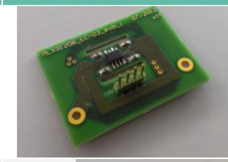 
PCB trace current **10-50A**	Single layer PCB with or without ferromagnetic shield (section 4.4.3).	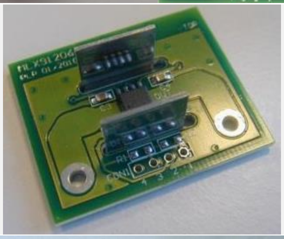
Bus bar **50-250A**	High field sensor with 12mm U-shaped ferromagnetic shield (section 4.4.4).	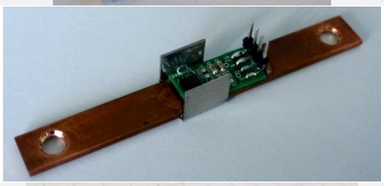
Bus bar **300-700A**	Very high field sensor with 12mm U-shaped ferromagnetic shield (section 4.4.5).	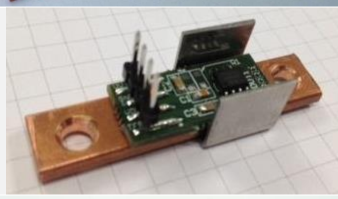
High dynamic range **50mA to 250A**	Dual range sensor with U-shaped and C-shaped shields (section 4.4.6).	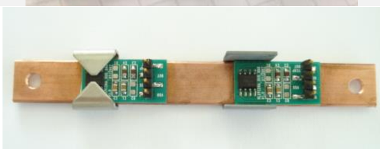
Non-intrusive current sensing from cable **10-100A**	Simple PCB with clamp-on shield wrapped around the cable (section 4.4.7).	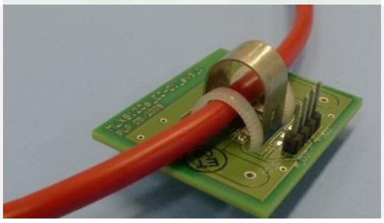

Table 4: Overview of the reference designs based on planar IMC-Hall® current sensors.

In the following sections, each solution is illustrated and described in details.

4.4.1 PCB application, 2-10A range, multi-layer/multi-turn solution

This solution is based on PCB with multiple layers and trace windings (current loops) for very high sensitivity. It can be used with or without ferromagnetic shield, depending on sensitivity and accuracy requirements. Figure 25 and Table 5 show the different designs and sensitivities achievable.

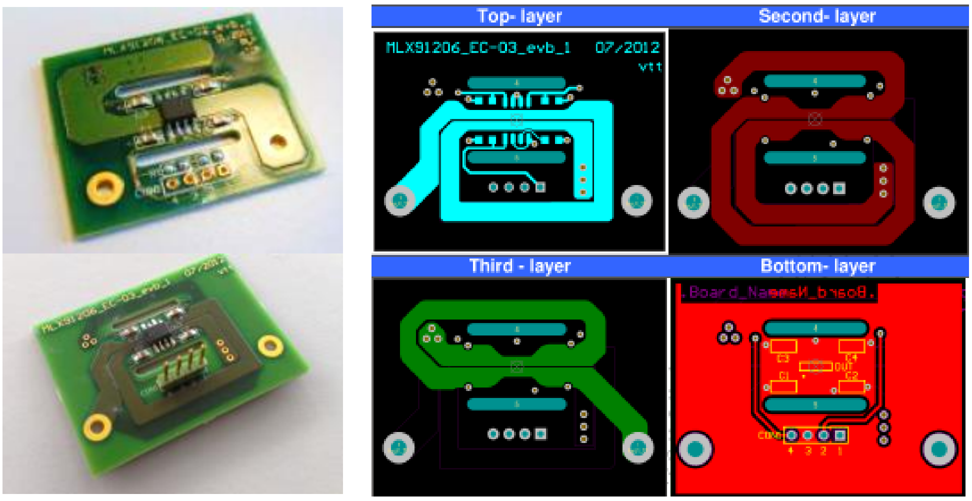

Figure 25: PCB layout example for very high sensitivity with 6 windings on 3 layers.

	3 windings without shield	3 windings with shield	6 windings without shield	6 windings with shield
Sensitivity (max) [mV/A]	210	350	420	700

Table 5: Maximum achievable sensitivities with the design shown in Figure 25.

4.4.2 PCB application, 2-10A range, ferromagnetic shield solution

This solution is based on a PCB with one layer and a single current trace (no windings). A closed ferromagnetic shield for high magnetic gain is used to boost the current sensitivity. Figure 26 shows the full system and some assembly details.

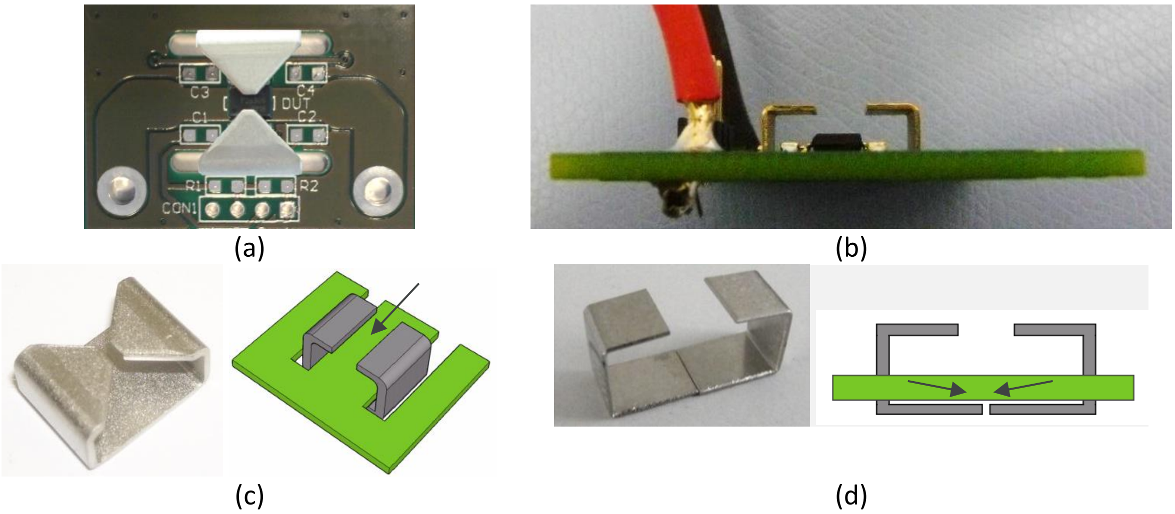

Figure 26: Top (a) and side (b) view of the full system. (c) Shield in one piece inserted through slots on the PCB edge. and (d) shield in two parts inserted in PCB slits and assembled together.

4.4.3 PCB application, 10-50A range

This solution is based on a PCB with one layer and a single current trace. It can be used with or without ferromagnetic shield (U-shaped). Two different sensitivity ranges are available: up to 60mV/A (without shield) or up to 170mV/A (with shield). Figure 27 shows the PCB with (a) and without shield. Figure 27.c shows how to assemble the shield on the PCB.

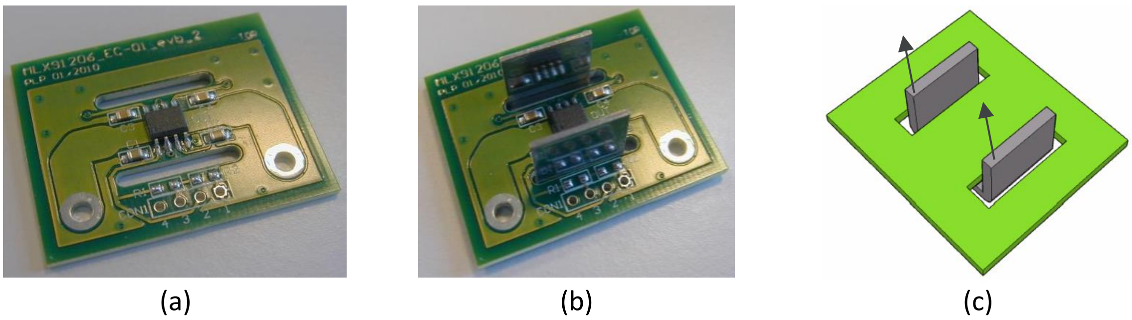

Figure 27: Single-layer evaluation board (a) without and (b) with shield. (c) Assembly instructions for shield.

4.4.4 Bus bar application, 50-250A range

This solution is based on the HF IMC sensor, that is mounted directly above the conductor on the PCB. A simple, low-cost and compact U-shaped shield is mounted around the sensor to protect it from stray fields and ensure good signal robustness against vibrations and displacements. With the dimensions shown here, the linearity error is lower than ± 1.5A for currents up to ±250A. Figure 28 shows the assembly detail, while Figure 29 shows the shield dimensions. Plot in Figure 30 shows an example of output voltage, with the linearity error.

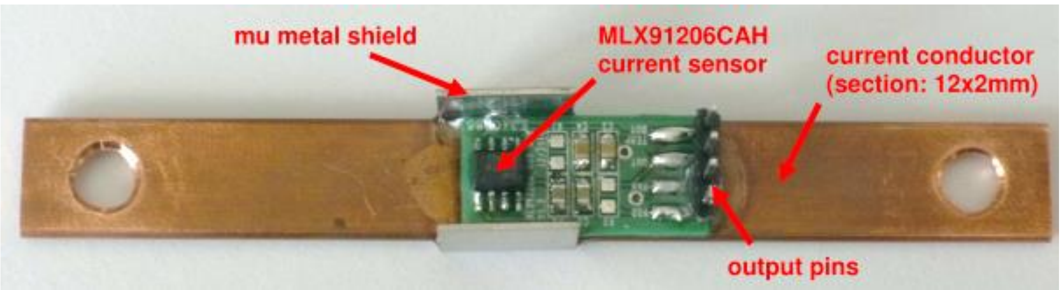

Figure 28: Demonstrator based on MLX91206 HF sensor and U12 shield with 0.8mm thickness.

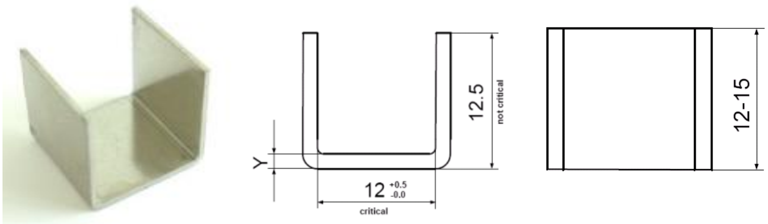

Figure 29: Shield dimensions.

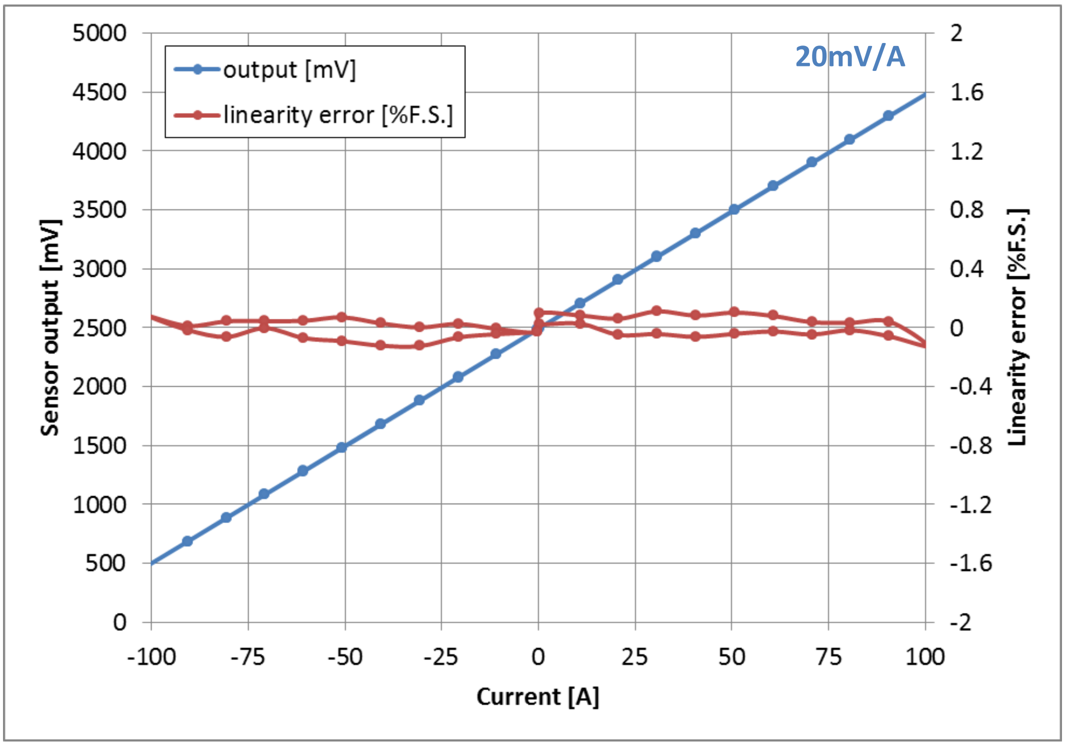

Figure 30: Typical output and non-linearity of a sensor calibrated for ±100A.

4.4.5 Bus bar application, 300-700A range

This solution is based on the use of a VHF IMC-Hall® sensor. The measurement range can be extended to 700A while keeping the same inner width than the one of the design described in 0, i.e. 12mm. To obtain a linearity up to 650A, the shield thickness must be adapted from 0.8 to 1.5mm. Figure 31 shows the assembly and the shield dimensions. This compact solution allows to measure up to 700A with a footprint of less than 2cm^2. Figure 32 shows the linearity error lower than ±5A for currents up to ±650A (i.e. no saturation of the signal).

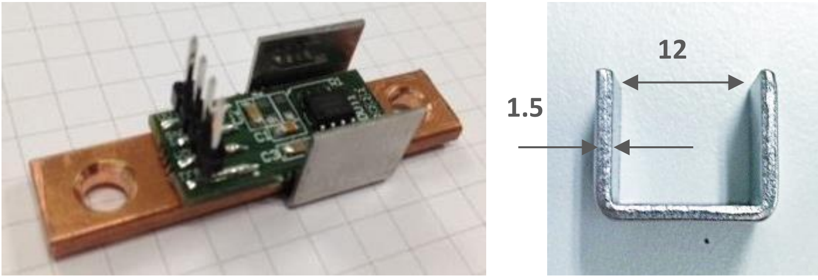

Figure 31: Demonstrator based on MLX91208 VHF sensor and U12 shield with 1.5mm thickness.

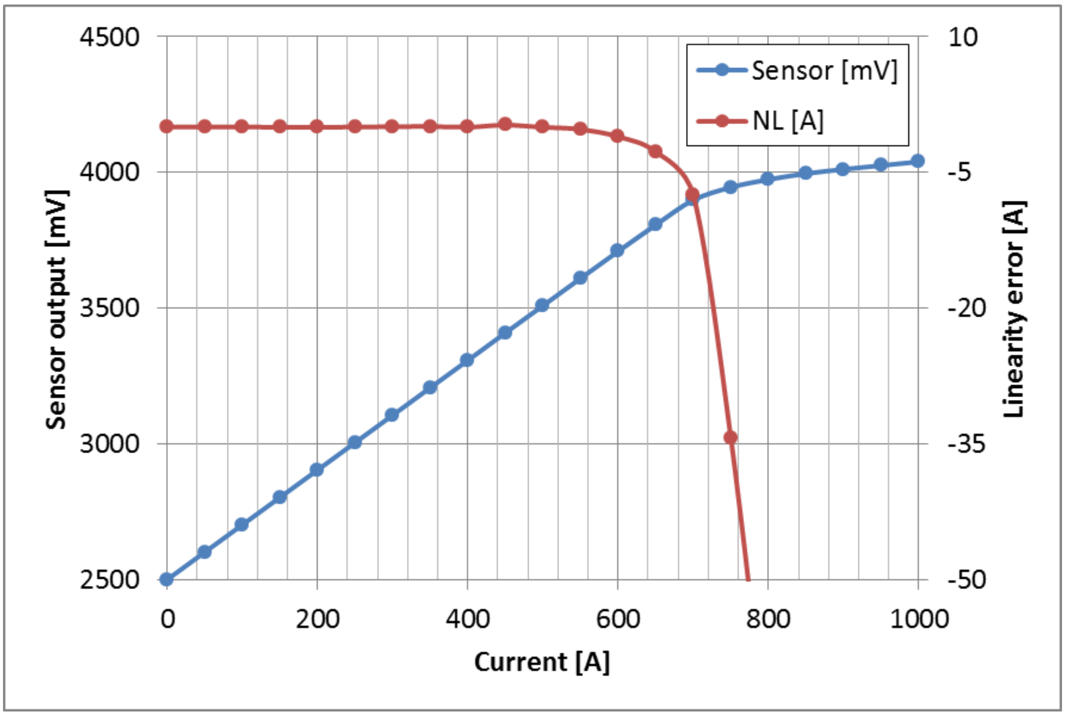

Figure 32: Sensor output and linearity error versus current.

4.4.6 Bus bar application, dual range 5A/200A

This solution allows applications with a wide dynamic range. One sensor with C-shaped (closed) shield is used for high accuracy at small currents (typical ±5A), while another sensor with U-shaped shield is used for high saturation limit (typical ±200A). Other combinations of ranges are possible depending on the application requirements. Figure 33 shows the assembly and shields geometry for this solution.

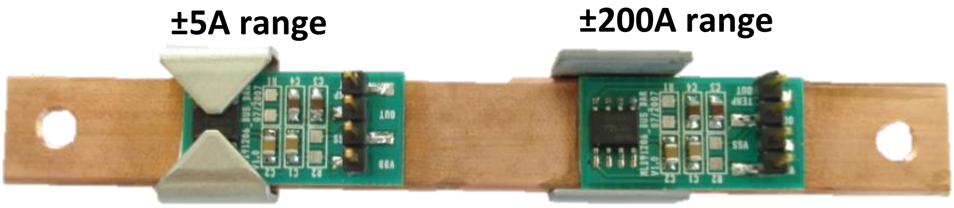

(a)

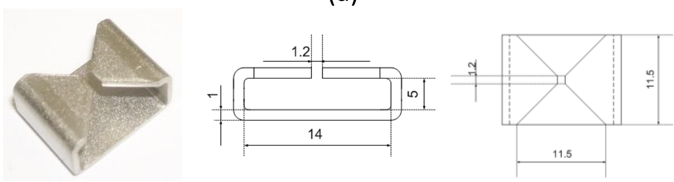

(b)

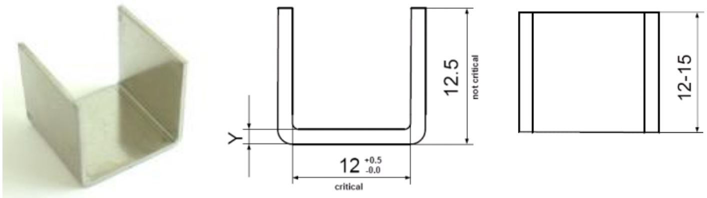

(c)

Figure 33: (a) Assembly. Images and sections for (b) closed shield and (c) U-shaped shield.

4.4.7 Cable application, 10-100A range

This solution is based on the clamp-on shield, that gathers the magnetic field around the cable and concentrates it above the sensor package. Small air gap ensures high magnetic gain. The shield geometry can be adapted to match various cable diameters and current ranges. Figure 34 shows the designs, while Figure 35 shows the real implementation of this concept.

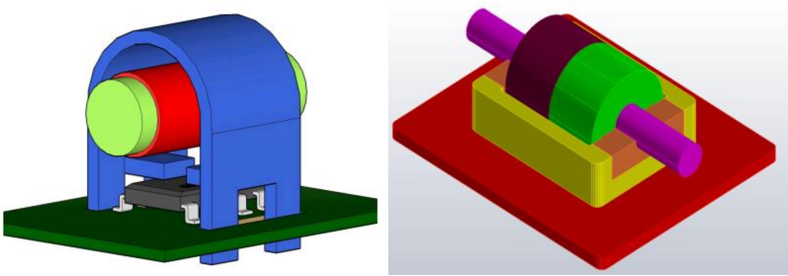

Figure 34: Cable clamp concepts (left: monolithic shield, right: two-part shield in plastic housing).

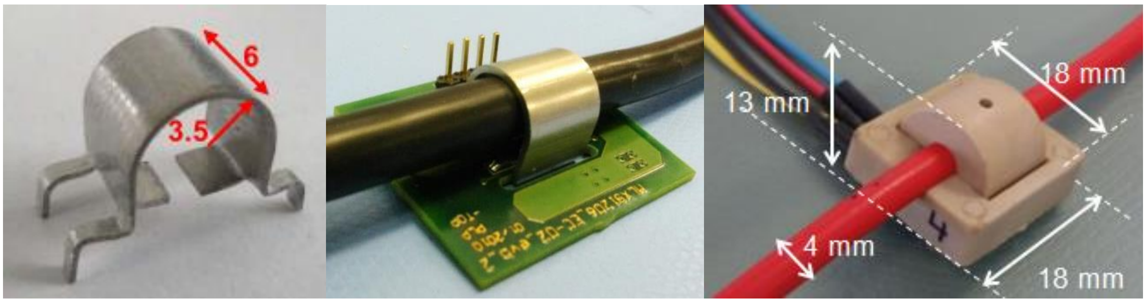

Figure 35: Implementation examples (monolithic and two-part shield in plastic housing).

Melexis has different IMC-Hall® sensors in its portfolio. The following section will introduce them, describing their specifications.

4.5 Quick Selection Guide

Melexis provides a list of sensors that can be selected for different applications (see Table 6). Each sensor can be bought with a factory trimmed sensitivity, using a specific option code. Sensitivity can be tuned according to customer needs.

	91208	91216	91218
Sensitivity [mV/mT] *			
▪ Extra High Field version (XHF)		20-125	12-115
▪ Very High Field version (VHF)	30-200	30-200	18-165
▪ High Field version (HF)	50-300	50-350	
▪ Low Field version (LF)	100-700		
Thermal sensitivity drift [%S]	±1.5	±1	±1.5
Thermal offset drift [mV]	±10	±5	±5
Bandwidth [kHz]	250	250	400
Noise	10 mVrms	6.5 mVrms	2 mVrms
Analog output	Yes	Yes	Yes
Programmable	Yes	Yes	Yes
Diagnostic functions			
▪ Over/Under-voltage detection	Yes	Yes	No
▪ Broken-track detection	No	Yes	No
▪ Clamping	No	Yes	No
▪ Over Current Detection	No	No	Yes
Possible supply voltages [V]	5	5	5, 3.3
Package	SOIC-8	SOIC-8	SOIC-8
Temp. range [°C]	-40 to 150		

Table 6: Main features and specifications of planar IMC-Hall® current sensors. Values are typical. See datasheets for maximum limits.

** Programmable*

Standard sensors are available in different option codes (Table 7). Updated list is available on datasheets.

Sensor	Option code	IMC version	Sensitivity range (typical) [mV/mT]
MLX91208	CAL-000	LF	100-700 (250)
	CAH-000	HF	50-300 (100)
	CAV-000	VHF	30-200 (40)
	CAV-001	VHF	30-200 (60)
MLX91216	ACH-000	HF	50-350 (100)
	ACV-000	VHF	30-200 (40)
	ACV-001	VHF	30-200 (60)
	ACV-002	VHF	30-200 (30)
	ACX-000	XHF	20-125 (25)
	ACX-001	XHF	20-125 (30)
	ACX-002	XHF	20-125 (20)
MLX91218	ARV-500	VHF	33.5-71 (40)
	ARX-501	XHF	20-40 (30)
	ARV-303*	VHF	22-35 (30)
	AFV-204**	VHF	47.5-165 (80)
	Generic VHF	VHF	18-165
	Generic XHF	XHF	12-115

Table 7: Option code and sensitivity range of planar IMC-Hall® current sensors (supply voltage equal to 5V unless otherwise specified). Please contact the Melexis sales department to have customized versions.

** Supply voltage 3.3V*

*** Fixed mode, supply voltage 3.3V*

Melexis provide a development kit for IMC-Hall® sensors. The application note is available on the website, at this link.

After the presentation of the two main technologies available with Melexis, the next sections will focus on the ferromagnetic materials selection, and on the calibration of sensors.

5 Ferromagnetic materials

This section introduces Melexis' main partners for ferromagnetic materials supply. Moreover, it introduces standard dimensions for shield and core ordering.

5.1 Ferromagnetic suppliers

Melexis partnered with MagLab for ferromagnetic components supply (Figure 36).

Figure 36: Logo and website of MagLab.

Section 5.2 is dedicated to shields, while section 5.3 is dedicated to cores. Section 5.4 shows the difference between the available ferromagnetic materials.

5.2 Ferromagnetic shields

5.2.1 U-Shield

Standard (U) and laminated (LU) shields can be ordered from the Maglab website using the following order codes convention (valid for both types). Figure 37 shows shields image and cross sections. Table 8 shows an example of shield ordering, and Table 9 shows different shield thicknesses.

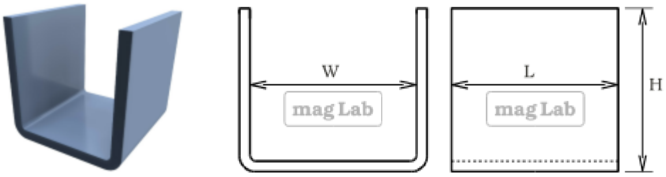

U (or LU) -Shield – Width – Length – Height – Thickness (– Ni)

Figure 37: Ordering information for the standard shield from MagLab.

Order code example	W [mm]	L [mm]	H [mm]	T [mm]
U (or LU) -Shield – 12 – 13 – 12.5 – 0.8	12	13	12.5	0.8

Table 8: Shield dimension convention for U-shields and LU-shields.

Material Specification	T [mm]	Ni [%]
Standard material	0.8	48
Other Thickness options	0.35 / 0.5 / 1 / 1.2	…

Table 9: Different thicknesses for U-shields.

We always suggest to use the standard shield dimensions, as this minimizes the fabrication costs and does not influence the final module performances.

5.2.2 Mechanical assembly

Ferromagnetic shields can be assembled by crimping, screwing or bonding (glue or tape). They can also be encapsulated in a pre-molded plastic case. The optimal solution depends on the application. In any case, care should be taken to avoid mechanical stress on the part of the shield involved in the magnetic measuring circuit. Figure 38 shows different solutions for shields assembly.

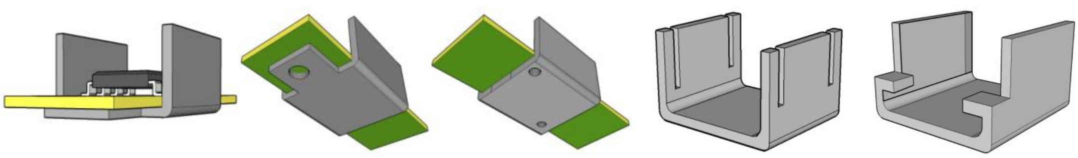

Figure 38: Several solutions for shield assembly.

One of the most common solutions is to use a pre-molded plastic case, with slots to insert the shields, as illustrated in Figure 39.

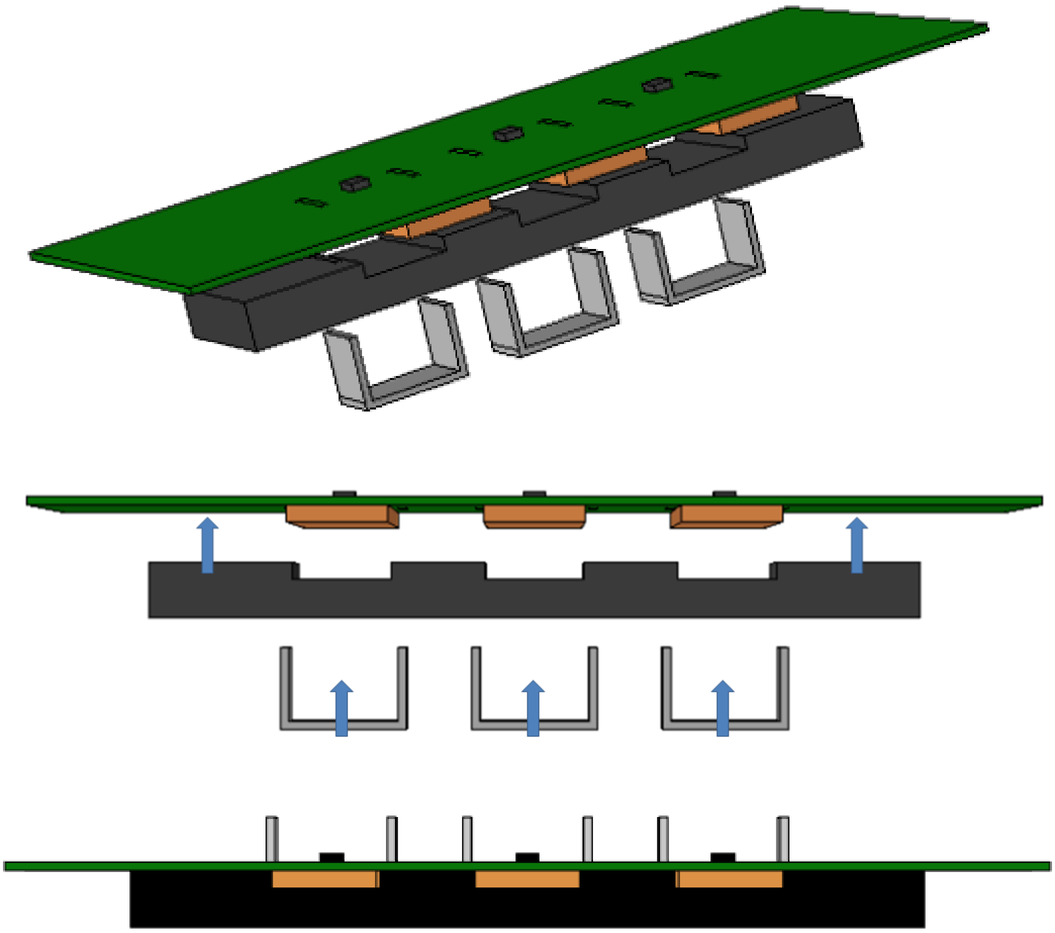

Figure 39: Assembly with pre-molded plastic case.

5.3 Ferromagnetic cores

Amorphous ferromagnetic cores can be ordered with the order codes convention shown in Figure 40. Table 10 shows an example of core order number.

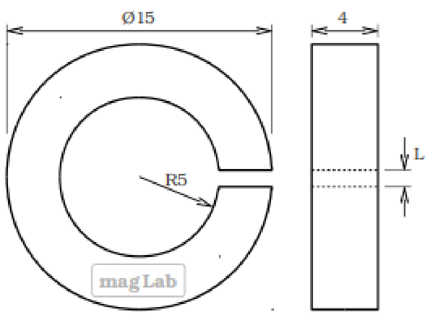

AMC1R5 – L

Figure 40: Amorphous ferromagnetic core sections, with ordering convention.

Order code example	L [mm]
AMC1R5 – 5	5

Table 10: Ordering example for amorphous ferromagnetic core.

Laminated cores can be ordered using the order codes convention shown in Figure 41. Table 11 shows an example of core order number.

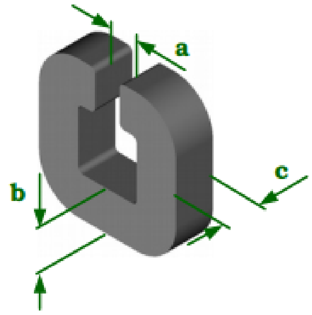

Ca – b – c

Figure 41: Ordering convention for laminated cores.

Order code example	a [mm]	b [mm]	c [mm]
C2.5 – 4 – 3.8	2.5	4	3.8

Table 11: Order code example for laminated cores.

Cores and shields are available in different ferromagnetic materials.

5.4 Ferromagnetic materials comparison

The performance of the current sensing solution relies on the careful selection of a proper core or shield material and manufacturing conditions (annealing, lamination, etc.).
Table 12 displays the main features of the most common material types.

Material	Price	Saturation field density B_{SAT}[T]	Hysteresis [%FS]
SiFe	$$	1.5	<0.25%
50% NiFe	$$$	1.3	<0.1%
ferrite	$	0.5	0.1%

Table 12: Features of most common ferromagnetic core materials.

6 End-of-line Calibration

Each current sensor is individually tested and calibrated over temperature in the Melexis production line. However, in order to achieve optimal accuracy, a final calibration is required at customer-side after assembly to compensate for mechanical tolerances (sensor position deviations, shield dimensions, etc.)
This final calibration can be done in two ways: either by using the Melexis tools to directly program the sensor EEPROM, or by adjusting the gain/offset at microcontroller level.

(a) (b) (c) (d)

Figure 42 resumes how the error are added. We can see that the mechanical assembly introduces an error in the field factor, that affect the total error. A final calibration will lower the error down to the case of the sensor after fabrication.Figure 1

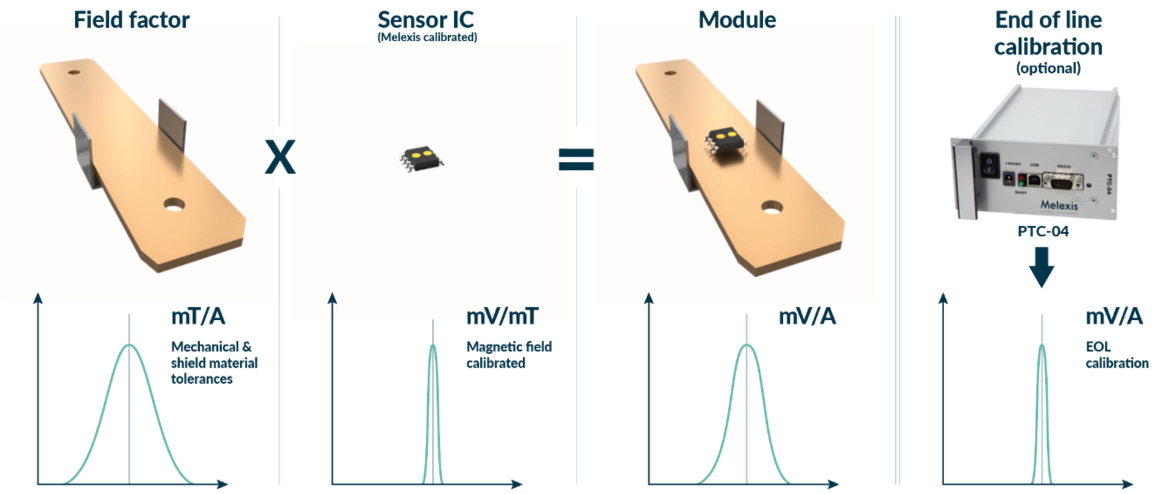

(a) (b) (c) (d)

Figure 42: Sum of error of sensor and mechanical assembly. We can see that the mechanical assemble (a) introduces an error that will affect the total error (c). An end of line calibration (d) will lower again the error to the value of the sensor after fabrication (b).

7 Additional information

Please refer to the following document for additional information on specific topics:

Typical cores and shield geometries
Standard designs of laminated and un-laminated U-shields and C-cores.

Current sensors programming and calibration
Different options available for customers in terms of sensor calibration.

8 Contact us

To get in contact with our current sensors application team, please fill and submit the technical inquiry form.

9 Disclaimer

The content of this document is believed to be correct and accurate. However, the content of this document is furnished "as is" for informational use only and no representation, nor warranty is provided by Melexis about its accuracy, nor about the results of its implementation. Melexis assumes no responsibility or liability for any errors or inaccuracies that may appear in this document. Customer will follow the practices contained in this document under its sole responsibility. This documentation is in fact provided without warranty, term, or condition of any kind, either implied or expressed, including but not limited to warranties of merchantability, satisfactory quality, non-infringement, and fitness for purpose. Melexis, its employees and agents and its affiliates' and their employees and agents will not be responsible for any loss, however arising, from the use of, or reliance on this document. Notwithstanding the foregoing, contractual obligations expressly undertaken in writing by Melexis prevail over this disclaimer.

This document is subject to change without notice, and should not be construed as a commitment by Melexis. Therefore, before placing orders or prior to designing the product into a system, users or any third party should obtain the latest version of the relevant information.
Users or any third party must determine the suitability of the product described in this document for its application, including the level of reliability required and determine whether it is fit for a particular purpose.

This document as well as the product here described may be subject to export control regulations. Be aware that export might require a prior authorization from competent authorities. The product is not designed, authorized or warranted to be suitable in applications requiring extended temperature range and/or unusual environmental requirements. High reliability applications, such as medical life-support or life-sustaining equipment or avionics application are specifically excluded by Melexis. The product may not be used for the following applications subject to export control regulations: the development, production, processing, operation, maintenance, storage, recognition or proliferation of:
1. chemical, biological or nuclear weapons, or for the development, production, maintenance or storage of missiles for such weapons;
2. civil firearms, including spare parts or ammunition for such arms;
3. defense related products, or other material for military use or for law enforcement;
4. any applications that, alone or in combination with other goods, substances or organisms could cause serious harm to persons or goods and that can be used as a means of violence in an armed conflict or any similar violent situation.

No license nor any other right or interest is granted to any of Melexis' or third party's intellectual property rights.

If this document is marked "restricted" or with similar words, or if in any case the content of this document is to be reasonably understood as being confidential, the recipient of this document shall not communicate, nor disclose to any third party, any part of the document without Melexis' express written consent. The recipient shall take all necessary measures to apply and preserve the confidential character of the document. In particular, the recipient shall (i) hold document in confidence with at least the same degree of care by which it maintains the confidentiality of its own proprietary and confidential information, but no less than reasonable care; (ii) restrict the disclosure of the document solely to its employees for the purpose for which this document was received, on a strictly need to know basis and providing that such persons to whom the document is disclosed are bound by confidentiality terms substantially similar to those in this disclaimer; (iii) use the document only in connection with the purpose for which this document was received, and reproduce document only to the extent necessary for such purposes; (iv) not use the document for commercial purposes or to the detriment of Melexis or its customers. The confidentiality obligations set forth in this disclaimer will have indefinite duration and in any case they will be effective for no less than 10 years from the receipt of this document.

This disclaimer will be governed by and construed in accordance with Belgian law and any disputes relating to this disclaimer will be subject to the exclusive jurisdiction of the courts of Brussels, Belgium.

The invalidity or ineffectiveness of any of the provisions of this disclaimer does not affect the validity or effectiveness of the other provisions.
The previous versions of this document are repealed.

IATF 16949 and ISO 14001 Certified